Published in final edited form as:
Cancer Res. 2008 August 1; 68(15): 6251–6259. doi:10.1158/0008-5472.CAN-08-0537.

Effect of ablation or inhibition of stromal matrix metalloproteinase-9 on lung metastasis in a breast cancer model is dependent on genetic background

Michelle D. Martin[*], **Kathy J. Carter**[*], **Sharon R. Jean-Philippe**[*], **Mayland Chang**[†], **Shahriar Mobashery**[†], **Sophie Thiolloy**[*], **Conor C. Lynch**[*,§], **Lynn M. Matrisian**[*], and **Barbara Fingleton**[*,#]

[*]Dept of Cancer Biology, Vanderbilt University Medical Center, Nashville TN 37232

[§]Dept of Orthopaedics & Rehabilitation, Vanderbilt University Medical Center, Nashville TN 37232

[†]Dept of Chemistry and Biochemistry and the Walther Cancer Research Center, University of Notre Dame, Notre Dame, IN 46556

Abstract

Matrix metalloproteinases (MMPs) are a family of enzymes with a myriad of functions. Lately we have come to realize that broad-spectrum inhibition of these enzymes, as was tried unsuccessfully in multiple phase III trials in cancer patients, is likely unwise given the pro- and anti-tumorigenic functions of various family members. Here we used the multistage mammary tumor model MMTV-PyVT to investigate roles for either MMP7 or MMP9 in tumor progression. We found no effect of genetic ablation of MMP7 or MMP9 on the multifocal tumors that developed in the mammary glands. Lack of MMP7 also had no effect on the development of lung metastases, suggesting that MMP7 is irrelevant in this model. In contrast, MMP9 deficiency was associated with an 80% decrease in lung tumor burden. The predominant cellular source of MMP9 was myeloid cells, with neutrophils being the largest contributor in tumor-bearing lungs. Experimental metastasis assays corroborated the role of host-derived MMP9 in lung metastasis and also facilitated determination of a time-frame most relevant for the MMP9-mediated effect. The lung tumors from MMP9-deficient mice showed decreased angiogenesis. Surprisingly, the anti-metastatic outcome of MMP9 ablation appeared to be dependent on strain. Only mice that had genetic background derived from C57BL/6 showed reduced metastasis, whereas mice fully of the FVB/N background showed no significant effect. These strain-specific responses were also observed in a study using a highly selective pharmacological inhibitor of MMP9 and thus suggest that responses to MMP inhibition are controlled by genetic differences.

Keywords

metalloproteinase; neutrophil; inhibitor; angiogenesis; lung metastasis

Introduction

The role of proteases in tumor progression has traditionally been viewed as limited to invasive ability, however that paradigm has been challenged in recent years by elegant *in vivo* studies, which have revealed multiple processes influenced by protease expression and function [1,2]

To whom reprint requests should be addressed: Dept of Cancer Biology VUMC, 771 PRB 2220 Pierce Ave, Nashville TN 37232-6840, Phone: 615 936-2913, Fax: 615 936-2911, Barbara.Fingleton@vanderbilt.edu.

These processes include tumor promotion, growth, angiogenesis, resistance to apoptosis, growth at secondary sites as well as invasive capabilities. In addition to awareness of an increased range of functions, there is also recognition of the array of different cell types that can produce proteases. Tumor cells, tumor-associated fibroblasts, endothelial cells and various cells of the myeloid and lymphoid classes have all been shown to supply certain proteolytic enzymes within a tumor microenvironment [1].

Various *in vivo* models of tumor progression have been used to illustrate functions of proteases [1,3]. Early studies indicated strong pro-tumorigenic roles and provided support for the clinical testing of pharmacological inhibitors of matrix metalloproteinases (MMPIs) in different cancers. Unfortunately, all phase III trials of such agents were unsuccessful [3,4]. One factor that must be considered is the misleading data obtained from preclinical mouse models. There is now a prevalent belief that complex genetic models that recapitulate the multistage nature of tumor progression and that allow more faithful representation of the heterogeneous nature of human tumors will be more predictive than the xenograft models that have generally been employed pre-clinically [5]. The mouse mammary tumor virus-driven polyoma viral oncogene (MMTV-PyVT) transgenic mouse model was originally generated in 1992 and the phenotype on the FVB/N strain described [6]. Briefly, the mice develop multifocal mammary tumors with an average latency of 35 days in the females. The tumors spontaneously metastasize to the lungs by ~90 days with a penetrance of 85%. The aggressive tumor phenotype in these mice is due to the multiple oncogenic pathways activated by the PyVT oncogene including src and PI3′kinase. The relevance of the MMTV-PyVT model to human breast cancer has been illustrated by both genetic and histologic studies [7,8], which indicated a strong similarity to stages of human ductal adenocarcinomas [8]. Microarray analysis identified a set of 16 genes in MMTV-PyvT tumors that matched 16 of the 17 genes proposed as a metastatic signature of human breast cancers [7]. We chose to use this model to ascertain the roles of the proteases MMP7 and MMP9 both in the setting of genetic ablation and following pharmacological inhibition.

Matrix metalloproteinase (MMP)-7 has frequently been described as an epithelial expressed protease and it is often strongly expressed by glandular epithelium of the intestine, stomach and prostate and in tumors arising from these cells [9,10]. Expression of MMP7 was reported in human breast cancers [11], including apparently normal breast glandular epithelium adjacent to tumors [12]. Targeting of MMP7 expression to mouse mammary glands using the MMTV promoter results in the development of hyperplastic lesions in multiparous females, while crossing MMTV-MMP7 mice to oncogenic MMTV-neu mice results in significant acceleration of the tumor phenotype in virgin females [13].

MMP9, also known as gelatinase B, has been associated with tumor progression in multiple studies [4,14]. In particular, several analyses show expression of MMP9 is a prognostic indicator in breast cancer patients [15-17]. As a type IV collagenase, it has been regarded as a critical enzyme for destruction of the basement membrane [18]. Some of the cell types expressing the highest levels of MMP9 are inflammatory cells such as neutrophils and macrophages [1,14,19].

Here we examine the effects of two different MMPs in the MMTV-PyVT model. Our results indicate that MMP7 is not significant in this model of mammary tumorigenesis, whereas MMP9 produced predominantly by inflammatory cells, is necessary for efficient development of metastases. Further, the contribution of MMP9 is strain-dependent as FVB/N mice show no effect of either genetic ablation or pharmacological inhibition of MMP9 on lung metastasis, in contrast to mice of the C57BL/6 strain. This has important ramifications for analysis of the effects of protease inhibition both in mouse models and in the genetically diverse human population.

Materials and Methods

Animals

All animal experiments animals were conducted following approval by the institutional animal use and care committee. *FVB/N-Tg (MMTV-PyVT)*^{634Mul} male mice were obtained from Jackson Research Labs (Bar Harbor, Maine) and crossed with either *mmp7*$^{-/-}$ or *mmp9*$^{-/-}$ females on the C57BL/6 background. F1 *PyVT/*$^{+}$ male pups were then mated to C57BL/6 *mmp7*$^{+/-}$ or *mmp9*$^{+/-}$ females to produce the study cohorts of F2 female *PyvT/+;mmp7*$^{-/-}$, *PyVT/*$^{+}$ *;mmp7*$^{+/+}$, *PyVT/*$^{+}$*;mmp9*$^{-/-}$ and *PyVT/*$^{+}$*;mmp9*$^{+/+}$animals. All *PyVT/*$^{+}$ *;mmp*$^{+/+}$ animals were littermates of the corresponding *PyVT/*$^{+}$*;mmp*$^{-/-}$ animals. Study mice were euthanized at 18 weeks, or earlier if tumor burden became too high. Study animals were palpated weekly and tumor diameters in two dimensions obtained using calipers. At necropsy, tumors were removed and a wet weight obtained for each. One tumor-filled gland was fixed in 10% buffered formalin for histological analysis. Lungs were inflated with 1.5 ml Bouin's fixative (Ricca Chemical, Arlington, TX) and removed for enumeration of surface metastases.

Rag2$^{-/-}$ mice (C57BL/6) were obtained from Taconic Farms Inc., Hudson, NY. Rag1$^{-/-}$ mice as well as MMP9$^{-/-}$ mice, both FVB/N, were kindly provided by Dr Lisa Coussens, Dept of Pathology, University of California San Francisco.

Histology

Lung tissues were embedded in paraffin and 5 μm-thick transverse sections cut and stained with hematoxylin-eosin. For assessment of tumor burden, the area of each section that was tumor, as well as the total tissue area, was measured using Metamorph (Universal Imaging Corp., Downington, PA) software. Four sections at depths 300μm apart were used for these analyses.

Immunohistochemistry

5 μm paraffin-embedded sections of lungs were assessed for expression of MMP-9 using rabbit anti-MMP9 (AbCam, Cambridge, MA), for macrophages using rat monoclonal anti- F4/80, and for neutrophils using a rat monoclonal anti-neutrophil antibody, both from AbD Serotec (Raleigh, NC). Expression of von Willebrand Factor (vWF) was detected using a rabbit anti-vWF antibody from Dako (Carpinteria, CA). Apoptosis levels were assessed by detection of cleaved caspase-3 (rabbit antibody from Cell Signaling Technology Inc., Danvers, MA) or TUNEL (Apoptag Plus Peroxidase kit, Millipore Corp., Billerica, MA) following manufacturers' protocols. Staining with a phosphohistone H3 antibody (Upstate Biologicals Inc., Lake Placid, NY) was used to assess proliferation.

Isolation and characterization of cell lines

Mammary tumors from MMTV-PyVT mice on the FVB/N background were minced and washed with DMEM containing fungizone (Invitrogen, Carlsbad, CA) and gentamycin (Invitrogen). The tumor pieces were plated in DMEM with 10% fetal calf serum plus antibiotics and incubated at 37°C in 5% CO_2 until tumor cells covered the dish. Single colonies were isolated, then expanded and characterized. Western blotting for E-cadherin and vimentin (antibodies from Sigma, St Louis, MO) confirmed epithelial origin of the clones. In order to assess their ability to grow in different organ microenvironments, cells from each line were injected into FVB/N mice in the mammary fat pad, tail vein or intra-tibially to assess orthotopic, pulmonary and bone growth, respectively. [n=3 for each organ site and cell line].

Luciferase expression

The 17L3C cell line was manipulated to express luciferase via a modified retroviral vector (from Dr. Swati Biswas, Vanderbilt University) in which a luciferase encoding gene was inserted into the multiple cloning site of the pMSCV vector (Clontech, Mountain View, CA). Phoenix packaging cells (a gift from Dr. Albert Reynolds, Vanderbilt University) were transfected using Superfect (Qiagen, Valencia, CA) according to the manufacturer. Virus was collected after 48 hours and used to transduce 17L3C cells. Selection media (containing 10μg/ml puromycin) was used for culturing clones of the 17L3C-luc cells. Luciferase expression was confirmed using the Luciferase Assay Reporter System (Promega, Madison, WI) before cells were injected into animals.

Experimental metastasis assays

$1 \times 10^6$17L3C-luc tumor cells were injected into the tail vein of 6-8 week old mice. After 21 days for the MMP9$^{-/-}$ imaging studies, and 14 days for the SB-3CT drug study, the mice were sacrificed, at which time the lungs were fixed in Bouin's solution. Lung tumors were then analyzed as above.

Bioluminescent imaging

The IVIS™ system (Caliper Life Sciences, Hopkinton, MA) was used to detect luminescence from 17L3C-luc cells after tail vein injection into mice. Mice were anesthetized using 2% isofluorane, and firefly luciferin (Gold Biotechnology, St. Louis, MO), 120mg/kg in PBS, delivered retro-orbitally 2 minutes prior to imaging. Mice were imaged at 4 hours after tumor cell inoculation and thereafter at fixed timepoints. Living Image™ software (Caliper) was used to quantify the change in luminescence intensity in the lungs over time.

Drug studies

The gelatinase-selective inhibitor SB-3CT [(4-phenoxyphenylsulfonyl) methylthiirane] [20] was stored as a powder at -20°C, and working solution was prepared fresh daily by dissolving in 1/10th volume of dimethylsulfoxide (DMSO; Sigma) and addition of water with constant stirring. The resultant suspension was injected intraperitoneally once daily at a dose of 50 mg/Kg. Control animals received equivalent volumes of 10% DMSO.

Statistical Analyses

All analysis was performed and graphs generated using Prism 4 software (GraphPad Software Inc., San Diego, CA). Comparisons between two groups used student's t test either with or without Welch's correction for unequal variance, as appropriate. Non-parametric data was compared using the Mann-Whitney test.

Results

Primary tumor growth is unaffected by MMP7 or MMP9 deficiency

To assess the contribution of either MMP9 or MMP7 to mammary tumor development, we crossed MMTV-PyVT mice on the FVB/N background with MMP9 or MMP7-null animals on the C57BL/6 background. Second-generation female littermates either wildtype or null with respect to the protease and all carrying a single PyVT allele were included in the study. Primary tumor characteristics assessed were time to appearance of the first palpable mammary mass (“tumor latency”), growth rate of the first tumor per mouse over time, number of mammary glands containing visible tumors (“multiplicity”) and total weight of all mammary tumors per animal (“tumor burden”). None of these parameters were affected by protease ablation [Fig 1A-D]. Additionally, the histological appearance of the mammary tumors was similar amongst

the different groups (data not shown). Hence, in this model of mammary tumorigenesis, neither MMP9 nor MMP7 play an essential role in primary tumor development.

Lung metastasis is attenuated in the absence of MMP9

Since the MMTV-PyVT tumor model shows development of spontaneous metastasis to the lungs, we next examined the tumor burden in the lungs of the protease-deficient mice and their wild-type littermates. This was done in 2 ways: first, by obtaining a surface tumor count; and second, by assessing tumor area in histological sections from multiple depths throughout the lungs.

In mice lacking MMP7, there was no difference in lung tumor burden in comparison to littermate controls (Fig 1E). Together with the primary tumor data, we conclude that in this mouse model of mammary tumor progression, MMP7 is a non-essential protease. In contrast, lack of MMP9 had a significant impact on development of lung metastasis with an 80% reduction in surface tumor number [wild-type median tumor number = 66.5; *mmp9*$^{-/-}$ median tumor number = 4] (Fig 1E). To further examine the metastatic lesions, we sectioned the lungs to obtain representative tissue from multiple depths. These were then assessed morphometrically to determine the percent area of lung parenchyma occupied by tumor lesions. Similarly to the gross surface counts, we observed a significant reduction in tumor burden in the lungs of MMP9-null MMTV-PyVT mice compared to the littermate controls (Supplemental Fig 1). The 76% reduction in total tumor area in the lungs correlated well with the 80% reduction in the number of surface tumor lesions. Morphometric analysis also allowed us to determine the tumor size in lungs from MMP9 wildtype or null MMTV-PyVT. Overall, the average tumor size in the MMP9-null animals was slightly but significantly smaller than seen in the littermate controls (Fig 1F) [mean ± standard deviation tumor area in wild-type = 0.25 ± 0.4 mm^2 vs 0.21 ± 0.02 mm^2 in MMP9$^{-/-}$].

Host MMP9 controls lung metastasis

To ascertain the cell types within primary and metastatic tumor foci that express MMP9, we performed immunohistochemical analysis. As can be seen in Fig 2A, tumor cells within the mammary gland were negative, whereas some infiltrating cells present in areas of necrosis or at the tumor periphery were positive. Based on appearance, we speculated that these cells were macrophages and neutrophils. In the lung tumor foci, many more MMP9-positive cells were apparent but again these appeared to be myeloid rather than tumor cells (Fig 2B). To confirm the identification of the cells expressing MMP9, we used double-staining immunofluorescence protocols with MMP9 and F4/80 antigen to identify macrophages, or an anti-neutrophil antibody to identify neutrophils (Fig 2C,D). While there were some MMP9-positive macrophages, the majority of MMP9-positive cells were identified as neutrophils (Fig 2C,D). Defects in neutrophil migration associated with MMP9 deficiency have been reported in some [21] but not all [22] model systems. In our samples, there was no difference between the number of neutrophils in the lungs of wild-type and MMP9-null MMTV-PyVT mice (data not shown), suggesting that MMP9 is not essential for neutrophil recruitment or migration to tumor-bearing lungs.

In order to verify the contribution of host MMP9 to the metastatic process, we turned to experimental metastasis assays. We first generated a series of cell lines from mammary tumors that developed in FVB/N MMTV-PyVT mice. The cell lines were characterized with respect to expression of the epithelial marker E-cadherin and lack of vimentin expression, and for their ability to grow in different *in vivo* organ environments. As listed in Supplemental Table 1, the three cell lines all show epithelial characteristics and are able to grow in different organ environments, albeit with differing growth kinetics. We have predominantly used the 17L3C cell line for our studies, however all *in vivo* experiments were repeated also with the R221A

line. These lines were transduced with a retroviral vector encoding luciferase to enable us to follow real time tumor growth *in vivo*.

Since the cell lines were derived from FVB/N mice and the MMP9$^{-/-}$ animals were on the C57BL/6 genetic background, we generated immunodeficient MMP9-null and wildtype controls by crossing the MMP9$^{-/-}$ mice with Rag2-null mice. Intravenous injection of 1×10^6 tumor cells into the tail vein of wildtype mice resulted in multiple lung tumors at the 3-week study termination point. In contrast, the same number of tumor cells in the MMP9-null mice resulted in a significant decrease in lung tumor burden (Fig 3A). In addition, the tumors in the MMP9$^{-/-}$ were significantly smaller than in the wildtype mice (Fig 3B). To determine at what time point MMP9 expression was critical, we used luciferase-labeled tumor cells and followed lung tumor burden over time. As can be seen in Fig 3C&D, luciferase activity was similar in wildtype and MMP9-null mice until approximately day 10 when the activity started to increase in the wildtype but remained relatively constant in the MMP9-null animals. Histological examination of lungs from mice at 21 days post injection confirmed a reduced tumor burden in the MMP9$^{-/-}$ animals [median tumors per mm^2 = 0.56 in wildtype mice, versus 0.34 in MMP9$^{-/-}$ mice].

Role of MMP9 in outgrowth of lung metastases

Since the imaging studies suggested that the effect of MMP9 in lung metastasis is evident at later stages of outgrowth rather than earlier survival as previously reported for lung adenocarcinomas [23], and we had observed a difference in the size of the lung tumor foci in the MMTV-PyVT wildtype vs MMP9$^{-/-}$ mice, we examined parameters of growth and death in the lungs. Both proliferation and apoptosis were significantly higher in the MMTV-PyVT;MMP9$^{+/+}$ animals than in those that were MMP9-null (Fig 4A,B). Although there were increases in both processes, the outcome should favor an overall increase in size, since proliferation is an exponential process. Similar changes in proliferation were seen with the experimental metastasis model (data not shown).

The increased proliferation and larger tumor size in the presence of MMP9 suggested that angiogenesis might be a relevant process. We used immunostaining for von Willebrand factor (vWF) to assess the levels of vasculature within lung tumor foci from both the spontaneous and experimental metastasis settings. Tumor sections from either the MMTV-PyVT (Fig 4C) or the tail vein-injected mice (Fig 4D), stained for vWF indicated significantly more blood vessels in the wildtype tumors. These data are in agreement with multiple reports from other model systems indicating a role for MMP9 in angiogenesis [19,24,25]. More specifically, our data are supportive of neutrophil-derived MMP9 being pro-angiogenic [19,26], however this is limited to the metastatic site in our model.

Requirement for MMP9 is strain-dependent

While performing experimental metastasis assays, we used both Rag2$^{-/-}$ mice on the C57BL/6 background as described above, as well as FVB/N mice, which are syngeneic with the PyVT cell lines. Surprisingly, MMP9$^{-/-}$ mice on the pure FVB/N background behaved similarly to wildtype mice with respect to lung tumor formation, as determined both by luciferase imaging and counting of surface tumors (Fig 5A-C). Furthermore, in a small study of the transgenic model MMTV-PyVT in MMP9$^{-/-}$ or wildtype mice of the FVB/N background we observed no significant effect on lung metastasis (5D). Hence, the MMP9-mediated effect is relevant in the C57BL/6 strain but not in the FVB/N strain.

One possible explanation for the difference between the strains is the amount or source of MMP9. However, the MMP9 expression pattern was not different. Additionally, the number of associated inflammatory cells was assessed in the lung tissues of MMTV-PyVT mice of the

FVB/N background compared to the mixed background. There was no statistical difference in the number of neutrophils present in tumor-bearing lungs between the two genetic backgrounds (data not shown).

MMP9 ablation phenotype is recapitulated by pharmacological inhibition

Since a differential effect of MMP9 gene deletion in development of both spontaneous and experimental lung metastasis is evident in C57BL/6, we wondered whether this resulted from null-mice never having had MMP9 from conception, or from a specific function of MMP9 in the metastatic process. We therefore used SB-3CT, a gelatinase-selective inhibitor that has previously been shown to attenuate tumor growth and metastasis in other models [20,27], to test whether pharmacological inhibition of MMP9 would show similar effects. In this study, we used immunocompromised mice ($Rag^{-/-}$) in either the FVB/N or C57BL/6 backgrounds. The mice were injected intravenously with luciferase-expressing 17L3C cells and imaged within 4 hours to ensure delivery of equivalent numbers of cells to lungs of all animals. The mice were then started on a regimen of daily injections of the drug SB-3CT or the corresponding vehicle for 14 days. During this period, the mice were imaged at days 3, 7 and 14 to assess tumor growth. As can be seen in Fig 6A and B, treatment of the C57BL/6 mice with the gelatinase inhibitor resulted in a significant attenuation of tumor growth in the lungs. In the FVB/N mice however, treatment with the inhibitor did not reduce tumor growth; in fact signal was enhanced (Fig 6C and D). Thus, as was seen in the null mice, pharmacological inhibition of MMP9 reduced lung tumor growth in C57BL/6 mice, but was ineffective or even stimulatory in FVB/N mice.

Discussion

Here we have examined the function of two proteases, MMP7 and MMP9, in a mouse model of spontaneously metastasizing breast cancer. Genetic ablation of either of these enzymes did not impact the development or growth of multifocal tumors in mammary glands. Lung metastasis was significantly attenuated in MMP9-null, but not MMP7-deficient animals. MMP9 was expressed in inflammatory cells, primarily neutrophils, in tumor-bearing lungs. Experimental metastasis assays allowed determination of a time-frame most relevant for the MMP9-mediated effect, which was in the later outgrowth stages of lung foci. In agreement with this observation, lung tumors from MMP9-deficient mice showed decreased angiogenesis. Surprisingly, the role of MMP9 appeared to be dependent on strain. In our studies, only mice that had significant genetic background derived from C57BL/6 showed reduced metastasis, whereas mice fully of the FVB/N background did not. These strain-specific responses were also observed in a study using a pharmacological inhibitor with high selectivity for MMP9, and thus suggest that tumor responses to MMP inhibition are controlled by genetic differences.

The function of several proteases from multiple enzyme families has now been investigated in the MMTV-PyVT model [28-31] This was a model identified by the Protease Consortium, a group of investigators with expertise in different protease families, as a valid setting for assessing differential contributions of proteases to multistage tumor development [32]. As with MMP9, two other proteases – uPA and plasminogen - were found to contribute to development of lung metastases, but not to mammary tumors [28,29]. In contrast, the cysteine protease cathepsin B, which is expressed by tumor cells and macrophages, contributed both to growth and progression of mammary tumors as well as to development of lung metastases [30]. A different pattern was seen with MMP14 (also known as MT1-MMP). In MMP14-null mammary glands, there was an increase in primary tumor growth rate, but this was followed by a reduction in lung metastasis [31]. The data suggested that MMP14 facilitated tumor dissemination by collagen cleavage in the peritumoral environment. There are multiple ways in which MMP9 could affect metastasis. MMP9 has been identified as a critical component

for priming of the "pre-metastatic niche", whereby soluble signals from a primary tumor result in selective preparation of certain organ sites to facilitate survival and growth of metastatic lesions in those organs [33,34]. Interestingly, we saw comparable effects irrespective of whether analyzing spontaneous metastasis or experimental metastasis, a result different to that reported by Hiratsuka et al., who reported effects of MMP9 ablation on metastasis only when a primary tumor was present [33]. Moreover, the imaging analysis suggested that the MMP9-mediated effect was more important in later stages of tumor outgrowth rather than initial survival of metastasizing cells. This interpretation is further suggested by the overall smaller size of the metastatic foci in MMP9$^{-/-}$ mice and the reduced vascular density. It should be remembered however, that we could only assess the temporal effect of MMP9 deletion in the experimental metastasis setting, where development of a pre-metastatic niche is not an issue. In the spontaneously metastasizing tumors of the MMTV-PyVT mice, it is possible that MMP9 contributes both to angiogenesis as our data indicates, but also to priming of a metastatic niche.

As has been reported in other settings [19,26], the primary source of MMP9 in these studies was cells of the myeloid lineage, particularly neutrophils. A previous analysis of MMTV-PyVT mice carrying a lacZ reporter driven by a region of the MMP9 promoter, suggested that mammary tumor cells express MMP9 at a timepoint corresponding to increased invasive activity [18]. We never saw any MMP9 expression by tumor cells, which may explain the lack of impact of MMP9 deficiency in the mammary glands. One potential reason for the disparate expression patterns is that the MMP9 promoter used in the lacZ analysis did not recapitulate the full *in vivo* promoter, including possible distant enhancer elements so that its expression pattern was not completely accurate.

The most surprising finding in our study was the influence of strain on the impact of MMP9 ablation. There are many reports of strain-related polymorphisms differentially affecting phenotypes [35], including cancer [36] in mouse models. Indeed, analysis of the phenotype of mice carrying the MMTV-PyVT transgene in different genetic backgrounds indicates a strong effect of strain on tumor aggressiveness in this model [37]. In particular, introduction of C57BL/6 increases tumor latency and extends the timing of metastasis to 120 days. The Hunter lab has invested a major effort in discovering potential host determinants of metastasis and have identified *Sipa1*, and *Rrp1b* as two genes, polymorphisms of which can impact susceptibility both in mice and humans [38-40]. Adding our results to their data further expands the pool of strain-specific metastasis modifiers, although it is not clear if *Mmp9* is itself the gene that is polymorphic. Indeed, analysis of strain-dependent modifiers of MMTV-PyVT metastasis indicated that chromosomes 6, 9, 13, 17 and 19 contained loci related to metastasis susceptibility [41], not chromosome 2 where *Mmp9* is located in the mouse.

Why MMP9 shows this strain dependent effect is unclear. The possibilities are that the enzyme itself, its relevant substrate in the lung environment or a modifier of its function is differentially regulated according to strain. When we examined neutrophil presence in the lungs of tumor-bearing mice, we detected no difference between the FVB/N and C57BL/6 backgrounds indicating that the primary source of MMP9 is not dissimilar. While we have identified the process of angiogenesis as the mechanism for the difference seen between MMP9 wild-type and null mice of the C57BL/6 strain, we have not determined the substrate responsible. It has been suggested that release of VEGF from matrix sequestration is one mechanism by which MMP9 promotes angiogenesis [24]. In a pilot study with the VEGF/VEGFR1 complex-detecting antibody [42] used in the Bergers study, we saw reduced complex formation in MMTV-PyVT; MMP9$^{-/-}$ lung tumors compared to controls (data not shown), suggesting that this is a possible explanation for the angiogenesis differences observed. Other roles for MMP9 in the angiogenic process include processing or liberation of other angiogenic growth factors [43]; degradation of basement membrane proteins to facilitate endothelial cell migration and tube formation [43]; and recruitment of pericytes to stabilize newly-formed vasculature [25].

In all our experiments in which FVB/N mice were used, deficiency of MMP9 or treatment with the gelatinase inhibitor SB-3CT appeared to be associated with enhanced tumor development. In the case of the MMP9$^{-/-}$ mice, this effect did not reach statistical significance, although a clear trend was evident (Fig 5). Following treatment with the inhibitor SB-3CT, a significant enhancement of luciferase signal, which corresponds to tumor burden, was seen. There have been reports previously of MMP9 ablation associated with enhanced tumor development. Coussens et al., reported that MMP9-null mice developed fewer, but more aggressive tumors in the K14-HPV16 skin cancer model [44]. Interestingly, these mice were also on the FVB/N background. In a model of lung metastasis of colonic tumor cells, Chen et al showed that use of the MMP-inhibiting agent doxycycline, which resulted in lower levels of MMP9, led to decreased numbers of metastatic foci, but those foci that did develop were larger and more vascularized [45]. Intriguingly, while there are multiple reports of increased MMP9 levels being a marker of poor prognosis, there is one clinical study suggesting that higher levels of MMP9 are associated with good prognosis in node-negative breast cancer [46]. This may reflect the heterogeneity with respect to MMP9 function that is related to genetic modifiers present in human populations, and has important implications for the treatment of metastatic breast cancer. Our data suggest that certain patients could respond to an MMP inhibitor by worsening disease progression while others show reduced metastatic growth. In seeming agreement with this idea, one MMPI inhibitor trial in small cell lung cancer was halted because patients treated with the drug were dying of their disease faster than were placebo-treated patients [4].

In conclusion, we have identified a metastasis-specific role for MMP9 in a transgenic mouse model of multistage mammary tumorigenesis that has been regarded as a credible model of human disease. The function of MMP9 appears to be in promotion of angiogenesis at the metastatic site; however this function is dependent on genetic background. MMP9 was a primary target of all synthetic MMPIs tested clinically in cancer patients, yet no successful inhibitor was identified. Our data would suggest that, while MMP9 may be a reasonable target, its contribution to tumor progression is highly influenced by genetic factors. The results from the drug studies reported here suggest that opposing results of MMP inhibition can be achieved i.e. more or fewer metastases, depending on genetic background. This finding clearly complicates interpretation of clinical studies of MMPIs and suggests that future clinical use of MMP9 inhibitors may depend on the identification of a “responsive haplotype” to allow selection of patients likely to respond.

Supplementary Material

Refer to Web version on PubMed Central for supplementary material.

Acknowledgments

We thank Dr Al Reynolds and Dr Swati Biswas of Vanderbilt University for reagents. We gratefully acknowledge Dr Lisa Coussens and Lidiya Korets at UCSF for generously providing us with multiple mouse lines.

Supported by R01CA84360 (to LMM) and by R01CA122417 (to MC and SM) from the NIH, and a subcontract (to BF) of the Breast Cancer Center of Excellence grant DAMD-17-02-1-0693 (to B. Sloane, Barbara Ann Karmanos Cancer Institute, Wayne State University, Detroit, MI 48201).

References

1. Egeblad M, Werb Z. New functions for the matrix metalloproteinases in cancer progression. Nat Rev Cancer 2002;2:161–74. [PubMed: 11990853]
2. Lynch CC, Matrisian LM. Matrix metalloproteinases in tumor-host cell communication. Differentiation 2002;70:561–73. [PubMed: 12492497]

3. Coussens LM, Fingleton B, Matrisian LM. Matrix metalloproteinase inhibitors and cancer: trials and tribulations. Science 2002;295:2387–92. [PubMed: 11923519]
4. Fingleton B. Matrix metalloproteinase inhibitors for cancer therapy: the current situation and future prospects. Exp Opin Therapeut Targets 2003;7:385–97.
5. Sharpless NE, Depinho RA. The mighty mouse: genetically engineered mouse models in cancer drug development. Nat Rev Drug Discov 2006;5:741–54. [PubMed: 16915232]
6. Guy CT, Cardiff RD, Muller WJ. Induction of mammary tumors by expression of polyomavirus middle T oncogene: a transgenic mouse model for metastatic disease. Mol Cell Biol 1992;12:954–61. [PubMed: 1312220]
7. Qiu TH, Chandramouli GV, Hunter KW, Alkharouf NW, Green JE, Liu ET. Global expression profiling identifies signatures of tumor virulence in MMTV-PyMT-transgenic mice: correlation to human disease. Cancer Res 2004;64:5973–81. [PubMed: 15342376]
8. Lin EY, Jones JG, Li P, et al. Progression to malignancy in the polyoma middle T oncoprotein mouse breast cancer model provides a reliable model for human diseases. Am J Pathol 2003;163:2113–26. [PubMed: 14578209]
9. Wielockx B, Libert C, Wilson C. Matrilysin (matrix metalloproteinase-7): a new promising drug target in cancer and inflammation? Cytokine Growth Factor Rev 2004;15:111–5. [PubMed: 15110795]
10. Wilson CL, Matrisian LM. Matrilysin: an epithelial matrix metalloproteinase with potentially novel functions. Int J Biochem Cell Biol 1996;28:123–36. [PubMed: 8729000]
11. Mylona E, Kapranou A, Mavrommatis J, Markaki S, Keramopoulos A, Nakopoulou L. The multifunctional role of the immunohistochemical expression of MMP-7 in invasive breast cancer. APMIS 2005;113:246–55. [PubMed: 15865605]
12. Fingleton B, Powell WC, Crawford HC, Couchman JR, Matrisian LM. A rat monoclonal antibody that recognizes pro- and active MMP-7 indicates polarized expression in vivo. Hybridoma (Larchmt) 2007;26:22–7. [PubMed: 17316082]
13. Rudolph-Owen LA, Chan R, Muller WJ, Matrisian LM. The matrix metalloproteinase matrilysin influences early-stage mammary tumorigenesis. Cancer Res 1998;58:5500–6. [PubMed: 9850086]
14. van Kempen LC, Rhee JS, Dehne K, Lee J, Edwards DR, Coussens LM. Epithelial carcinogenesis: dynamic interplay between neoplastic cells and their microenvironment. Differentiation 2002;70:610–23. [PubMed: 12492502]
15. Wu ZS, Wu Q, Yang JH, et al. Prognostic significance of MMP-9 and TIMP-1 serum and tissue expression in breast cancer. Int J Cancer 2008;122:2050–6. [PubMed: 18172859]
16. Hanemaaijer R, Verheijen JH, Maguire TM, et al. Increased gelatinase-A and gelatinase-B activities in malignant vs benign breast tumors. Int J Cancer 2000;86:204–7. [PubMed: 10738247]
17. Mylona E, Nomikos A, Magkou C, et al. The clinicopathological and prognostic significance of membrane type 1 matrix metalloproteinase (MT1-MMP) and MMP-9 according to their localization in invasive breast carcinoma. Histopathology 2007;50:338–47. [PubMed: 17257129]
18. Kupferman ME, Fini ME, Muller WJ, Weber R, Cheng Y, Muschel RJ. Matrix metalloproteinase 9 promoter activity is induced coincident with invasion during tumor progression. Am J Pathol 2000;157:1777–83. [PubMed: 11106549]
19. Nozawa H, Chiu C, Hanahan D. Infiltrating neutrophils mediate the initial angiogenic switch in a mouse model of multistage carcinogenesis. Proc Natl Acad Sci U S A 2006;103:12493–8. [PubMed: 16891410]
20. Kruger A, Arlt MJ, Gerg M, et al. Antimetastatic activity of a novel mechanism-based gelatinase inhibitor. Cancer Res 2005;65:3523–6. [PubMed: 15867341]
21. Khandoga A, Kessler JS, Hanschen M, et al. Matrix metalloproteinase-9 promotes neutrophil and T cell recruitment and migration in the postischemic liver. J Leukoc Biol 2006;79:1295–305. [PubMed: 16551680]
22. Felkel C, Scholl U, Mader M, et al. Migration of human granulocytes through reconstituted basement membrane is not dependent on matrix metalloproteinase-9 (MMP-9). J Neuroimmunol 2001;116:49–55. [PubMed: 11311329]
23. Acuff HB, Carter KJ, Fingleton B, Gorden DL, Matrisian LM. Matrix metalloproteinase-9 from bone marrow-derived cells contributes to survival but not growth of tumor cells in the lung microenvironment. Cancer Res 2006;66:259–66. [PubMed: 16397239]

24. Bergers G, Brekken R, McMahon G, et al. Matrix metalloproteinase-9 triggers the angiogenic switch during carcinogenesis. Nat Cell Biol 2000;2:737–44. [PubMed: 11025665]
25. Chantrain CF, Shimada H, Jodele S, et al. Stromal matrix metalloproteinase-9 regulates the vascular architecture in neuroblastoma by promoting pericyte recruitment. Cancer Res 2004;64:1675–86. [PubMed: 14996727]
26. Ardi VC, Kupriyanova TA, Deryugina EI, Quigley JP. Human neutrophils uniquely release TIMP-free MMP-9 to provide a potent catalytic stimulator of angiogenesis. Proc Natl Acad Sci USA 2007;104:20262–7. [PubMed: 18077379]
27. Bonfil RD, Sabbota A, Nabha S, et al. Inhibition of human prostate cancer growth, osteolysis and angiogenesis in a bone metastasis model by a novel mechanism-based selective gelatinase inhibitor. Int J Cancer 2006;118:2721–6. [PubMed: 16381009]
28. Bugge TH, Lund LR, Kombrinck KK, et al. Reduced metastasis of Polyoma virus middle T antigen-induced mammary cancer in plasminogen-deficient mice. Oncogene 1998;16:3097–104. [PubMed: 9671388]
29. Almholt K, Lund LR, Rygaard J, et al. Reduced metastasis of transgenic mammary cancer in urokinase-deficient mice. Int J Cancer 2005;113:525–32. [PubMed: 15472905]
30. Vasiljeva O, Papazoglou A, Kruger A, et al. Tumor cell-derived and macrophage-derived cathepsin B promotes progression and lung metastasis of mammary cancer. Cancer Res 2006;66:5242–50. [PubMed: 16707449]
31. Szabova L, Chrysovergis K, Yamada SS, Holmbeck K. MT1-MMP is required for efficient tumor dissemination in experimental metastatic disease. Oncogene. 2007epub ahead of print
32. Giranda VL, Matrisian LM. The protease consortium: an alliance to advance the understanding of proteolytic enzymes as therapeutic targets for cancer. Molec Carcinogen 1999;26:139–42.
33. Hiratsuka S, Nakamura K, Iwai S, et al. MMP9 induction by vascular endothelial growth factor receptor-1 is involved in lung-specific metastasis. Cancer Cell 2002;2:289–300. [PubMed: 12398893]
34. Kaplan RN, Riba RD, Zacharoulis S, et al. VEGFR1-positive haematopoietic bone marrow progenitors initiate the pre-metastatic niche. Nature 2005;438:820–7. [PubMed: 16341007]
35. Bult CJ, Eppig JT, Kadin JA, Richardson JE, Blake JA. The Mouse Genome Database (MGD): mouse biology and model systems. Nucleic Acids Res 2008;36:D724–8. [PubMed: 18158299]
36. Dragani TA. 10 years of mouse cancer modifier loci: human relevance. Cancer Res 2003;63:3011–8. [PubMed: 12810618]
37. Lifsted T, Le Voyer T, Williams M, et al. Identification of inbred mouse strains harboring genetic modifiers of mammary tumor age of onset and metastatic progression. Int J Cancer 1998;77:640–4. [PubMed: 9679770]
38. Park YG, Zhao X, Lesueur F, et al. Sipa1 is a candidate for underlying the metastasis efficiency modifier locus Mtes1. Nat Genet 2005;37:1055–62. [PubMed: 16142231]
39. Crawford NP, Ziogas A, Peel DJ, Hess J, Anton-Culver H, Hunter KW. Germline polymorphisms in SIPA1 are associated with metastasis and other indicators of poor prognosis in breast cancer. Breast Cancer Res 2006;8:R16. [PubMed: 16563182]
40. Crawford NP, Qian X, Ziogas A, et al. Rrp1b, a new candidate susceptibility gene for breast cancer progression and metastasis. PLoS Genet 2007;3:e214. [PubMed: 18081427]
41. Hunter KW, Broman KW, Voyer TL, et al. Predisposition to efficient mammary tumor metastatic progression is linked to the breast cancer metastasis suppressor gene Brms1. Cancer Res 2001;61:8866–72. [PubMed: 11751410]
42. Brekken RA, Huang X, King SW, Thorpe PE. Vascular endothelial growth factor as a marker of tumor endothelium. Cancer Res 1998;58:1952–9. [PubMed: 9581838]
43. van Hinsbergh VW, Engelse MA, Quax PH. Pericellular proteases in angiogenesis and vasculogenesis. Arterioscler Thromb Vasc Biol 2006;26:716–28. [PubMed: 16469948]
44. Coussens LM, Tinkle CL, Hanahan D, Werb Z. MMP-9 supplied by bone marrow-derived cells contributes to skin carcinogenesis. Cell 2000;103:481–90. [PubMed: 11081634]
45. Chen X, Su Y, Fingleton B, et al. Increased plasma MMP9 in integrin alpha1-null mice enhances lung metastasis of colon carcinoma cells. Int J Cancer 2005;116:52–61. [PubMed: 15756690]

46. Scorilas A, Karameris A, Arnogiannaki N, et al. Overexpression of matrix-metalloproteinase-9 in human breast cancer: a potential favourable indicator in node-negative patients. Brit J Cancer 2001;84:1488–96. [PubMed: 11384099]

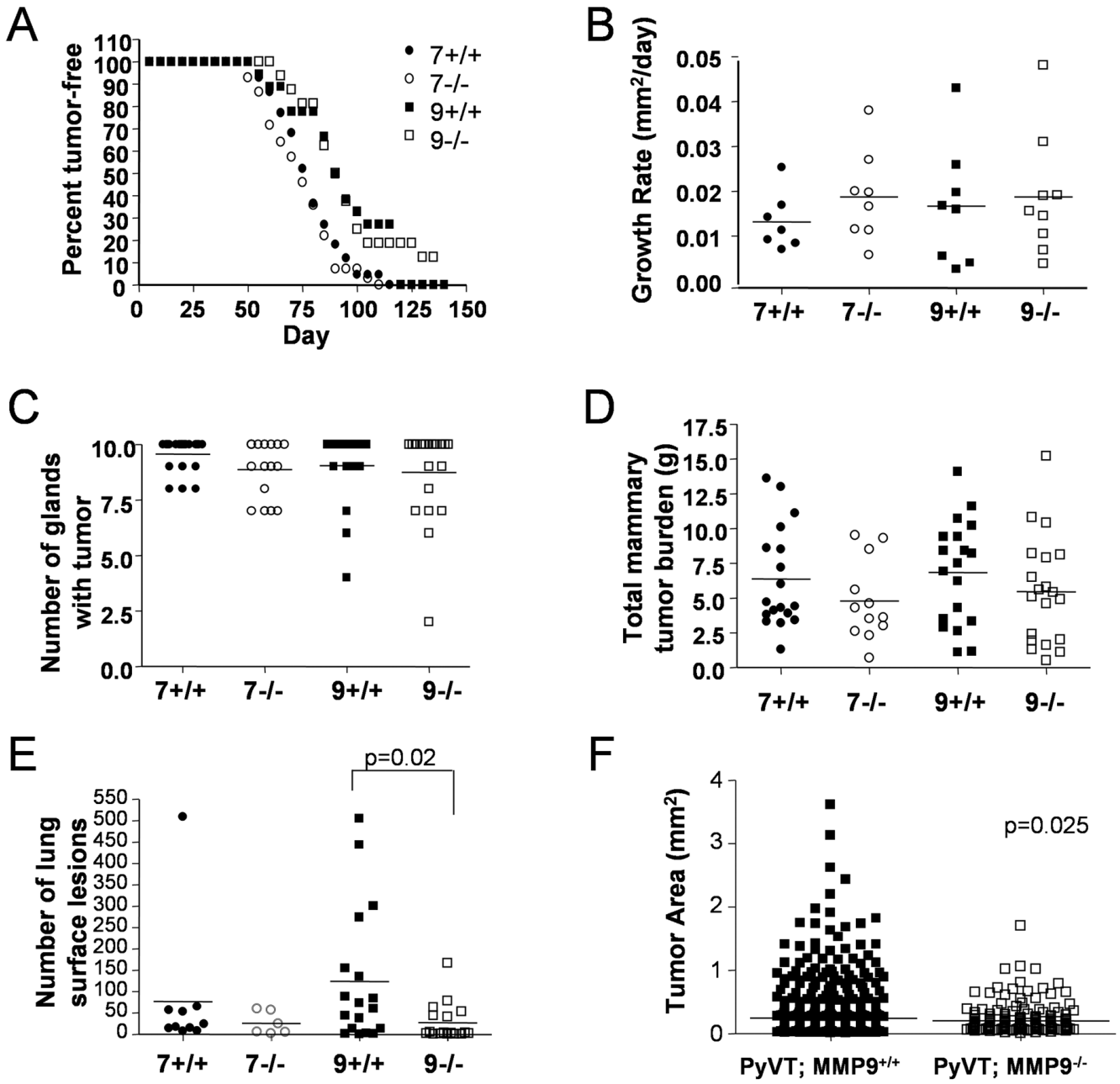

Figure 1.

(A) Tumor-latency curves for MMTV-PyVT; MMP7-/-, (clear circles) MMTV-PyVT; MMP9$^{-/-}$ (clear squares) mice and their corresponding littermate MMTV-PyVT; MMP$^{+/+}$ (filled circles) and MMTV-PyVT; MMP9$^{+/+}$ (filled squares) controls. For each set, the wild-type and corresponding null groups overlap each other. (B) Growth rate of the first palpable mammary tumor arising in MMTV-PyVT; MMP7$^{+/+}$ (n=7), MMTV-PyVT; MMP7$^{-/-}$ (n=8); MMTV-PyVT; MMP9$^{+/+}$ (n=8) and MMTV-PyVT; MMP9$^{-/-}$ (n=9) mice. (C) Number of mammary glands with frank tumors at time of sacrifice in MMTV-PyVT; MMP7$^{+/+}$ (n=18), MMTV-PyVT; MMP7$^{-/-}$ (n=12); MMTV-PyVT; MMP9$^{+/+}$ (n=19) and MMTV-PyVT; MMP9$^{-/-}$ (n=20) mice. (D) Total mammary tumor burden (wet weight) of MMTV-PyVT; MMP7$^{+/+}$ (n = 18), MMTV-PyVT; MMP7$^{-/-}$ (n=12); MMTV-PyVT; MMP9$^{+/+}$ (n=19) and

MMTV-PyVT; MMP9$^{-/-}$ (n=20) mice. (E) Number of tumor foci evident on lung surfaces of MMTV-PyVT; MMP7$^{+/+}$ (filled circles, n = 10), MMTV-PyVT; MMP7$^{-/-}$ (n=6); MMTV-PyVT; MMP9$^{+/+}$ (n=18) and MMTV-PyVT; MMP9$^{-/-}$ (n=17) mice. (F) Area of each histologically-identified tumor in lungs of MMTV-PyVT; MMP9+/+ (n = 795 tumors in 12 mice) and MMTV-PyVT; MMP9-/- (n=188 tumors in 10 mice) mice. Note: all four groups of animals are shown on single graphs for ease of visualization, however statistical analysis only compared each null group with the appropriate wild-type control littermate group.

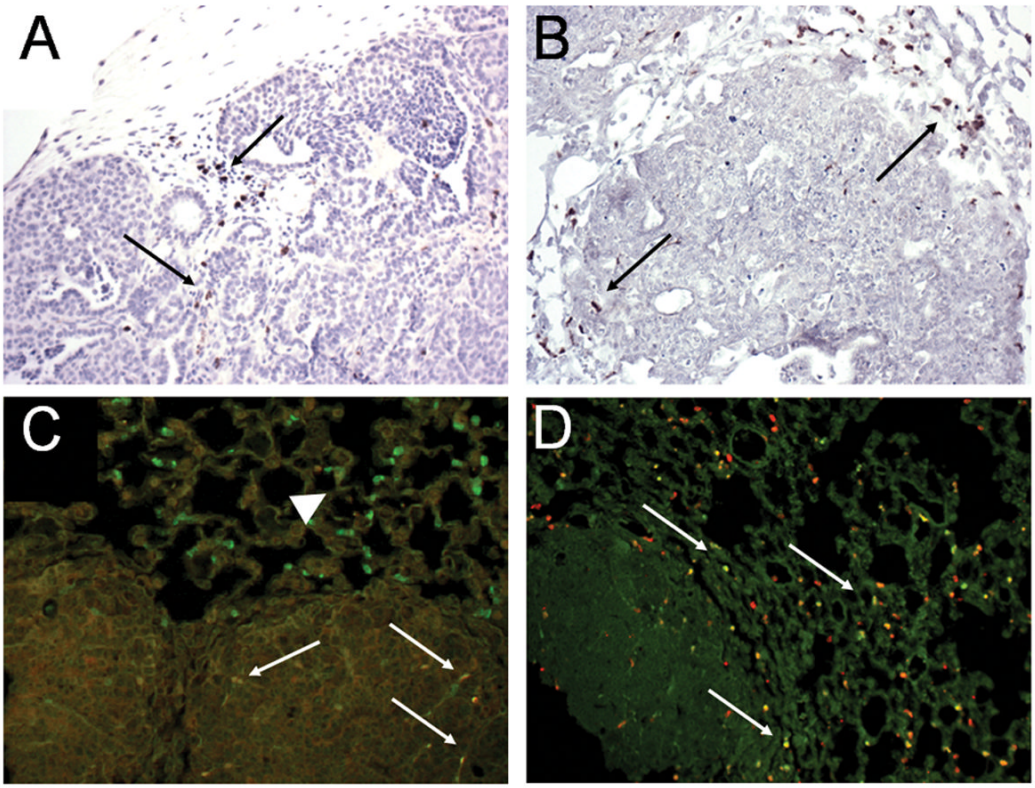

Figure 2.
Immunohistochemical staining for MMP9 in sections of mammary tumor (A) and lung tumor (B) of MMTV-PyVT; $MMP9^{+/+}$ mouse. Arrows indicate positively-stained cells. (200X magnification). (C) Immunofluorescent staining of macrophages (red) and MMP9 (green) in lung tumor of MMTV-PyVT; $MMP9^{+/+}$ mouse. Arrows indicate dual staining while arrowhead indicates significant MMP9 positivity in surrounding cells that are not macrophages. (200× magnification). (D) Immunofluorescent staining of neutrophils (red) and MMP9 (green) in lung tumor of MMTV-PyVT; $MMP9^{+/+}$ mouse. (200× magnification). Note that the majority of positive cells are dual-stained.

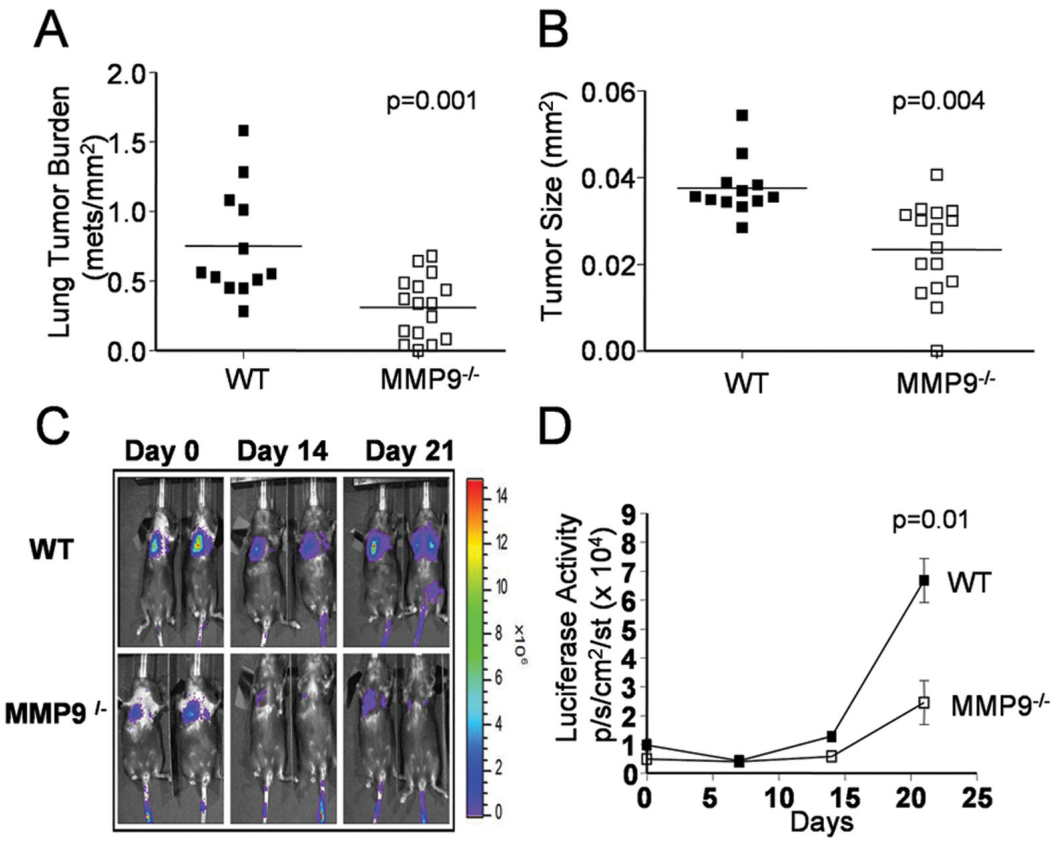

Figure 3.

(A) Lung tumor burden in wild-type and MMP9$^{-/-}$ Rag2-null mice injected with via the tail vein 1×10^6 17L3C PyVT tumor cells and sacrificed after 3 weeks. Tumor burden was assessed histologically. (B) Size of tumors in lungs of wild-type and MMP9$^{-/-}$ Rag2-null mice injected via the tail vein with 1×10^6 17L3C PyVT tumor cells and sacrificed after 3 weeks. (C) Representative images of luciferase activity overlaid on photographs of wild-type (WT) or MMP9-/- Rag2-null mice. Images were generated using the IVIS imaging system as stated in Materials and Methods. (D) Luciferase activity as measured by IVIS over time in wild-type (WT) and MMP9-/- Rag2-null mice that had been injected with 1×10^6 17L3C-luc cells.

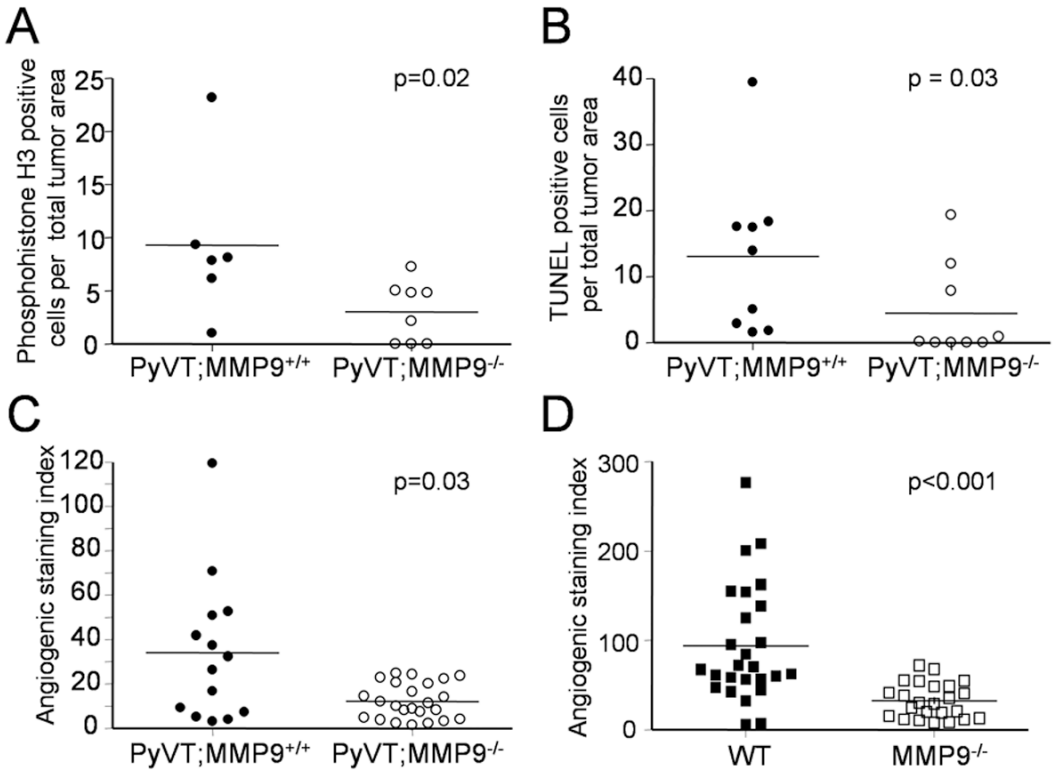

Figure 4.

(A) Phosphohistone H3 immunostaining in lung tumors from MMTV-PyVT; $MMP9^{+/+}$ (n=6) and MMTV-PyVT; $MMP9^{-/-}$ (n=8) mice. (B) TUNEL staining in lung tumors from MMTV-PyVT; $MMP9^{+/+}$ (n=9) and MMTV-PyVT; $MMP9^{-/-}$ (n=9) mice. (C) Immunostaining for vWF in individual lung tumors of MMTV-PyVT; $MMP9^{+/+}$ (n=14 tumors from 4 mice) and MMTV-PyVT; $MMP9^{-/-}$ (n=24 from 5 mice) animals. (D) Immunostaining for vWF in individual lung tumors of wild-type (WT; n= 26 tumors from 3 mice) and $MMP9^{-/-}$ (n= 24 tumors from 4 mice) Rag2-null mice that had been injected with 1×10^6 17L3Cluc cells 21 days previously via the tail vein.

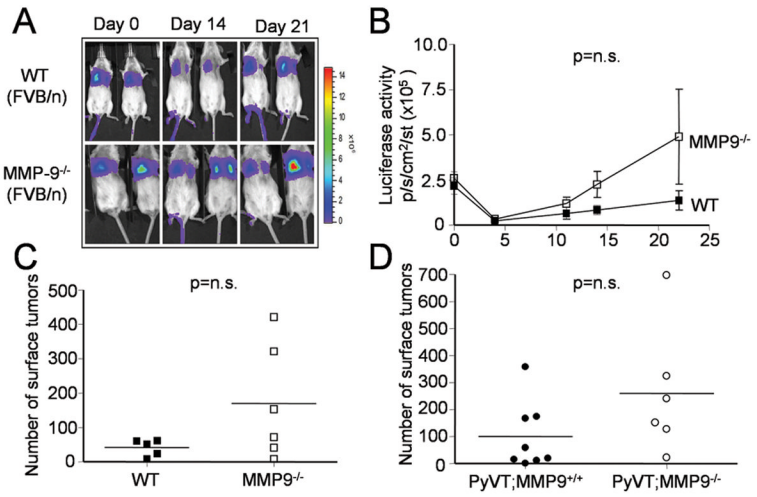

Figure 5.

(A) Representative images of luciferase activity overlaid on photographs of wild-type (WT) or MMP9-/- mice in the FVB/N background. (B) Luciferase activity as measured by IVIS over time in wild-type (WT, n=5) and MMP9$^{-/-}$ (n=6) mice in FVB/N background that had been injected with 1×10^{6} 17L3C-luc cells. (C) Number of tumor foci evident on the lung surfaces of wild-type (WT) or MMP9$^{-/-}$ mice in the FVB/N background 3 weeks intravenous tumor injection. (D) Number of tumor foci evident on the lung surfaces of MMTV-PyVT; MMP9$^{-/-}$ (n=8) or MMTV-PyVT;MMP9$^{+/+}$ (n=6) mice in the FVB/N at time of sacrifice (14 weeks).

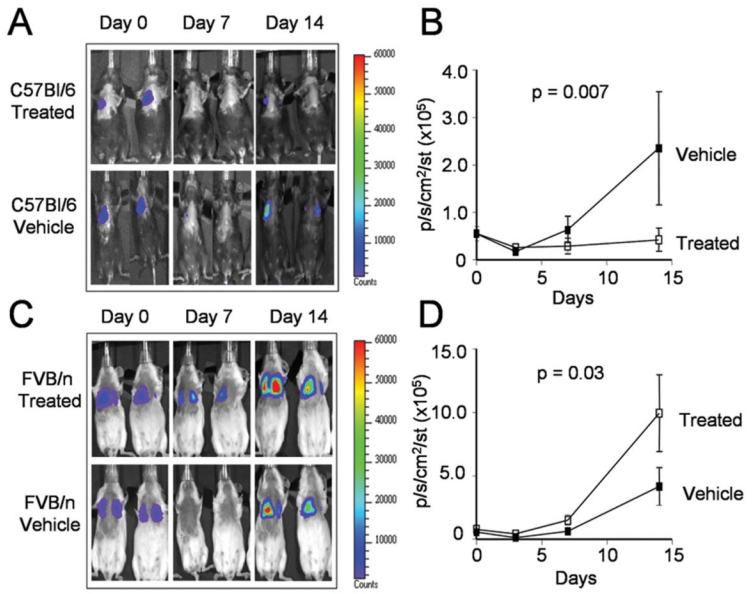

Figure 6.

(A) Luciferase imaging of tumor growth in immunodeficient ($Rag2^{-/-}$) C57BL/6 mice treated with the gelatinase inhibitor SB-3CT or vehicle (10% DMSO) following intravenous injection of 1×10^6 17L3Cluc tumor cells. (B) Graphical representation of the change in luciferase activity, indicative of tumor burden, over time in the tumor-injected C57BL/6 mice exposed to the gelatinase inhibitor SB-3CT (n=5) or vehicle control (n=2). (C) Luciferase imaging of tumor growth in immunodeficient ($Rag1^{-/-}$) FVB/N mice treated with the gelatinase inhibitor SB-3CT or vehicle following intravenous injection of 1×10^6 17L3Cluc tumor cells. (D) Graphical representation of the change in luciferase activity, indicative of tumor burden, over time in the tumor-injected FVB/N mice exposed to the gelatinase inhibitor SB-3CT (n=5) or vehicle control (n=5). Note the drug-treated mice show increased luciferase activity.